IIETA International Information and Engineering Technology Association
Advancing the World of Information and Engineering

Mathematical Modelling of Engineering Problems
Vol. 13, No. 3, March, 2026, pp. 541-554
Journal homepage: http://iieta.org/journals/mmep

Enhancement of Robotics Networks Cooperative Based on Route Planning and Target Detection for Unmanned Aerial Vehicles and Autonomous Surface Vehicles

Ammar Abdul Ameer Rasheed[1], Ali Majeed Mahmood[2*]

[1] College of Computer Engineering, University of Technology-Iraq, Baghdad 10066, Iraq
[2] College of Artificial Intelligence Engineering, University of Technology-Iraq, Baghdad 10066, Iraq

Corresponding Author Email: Ali.M.Mahmood@uotechnology.edu.iq

https://doi.org/10.18280/mmep.130309

Received: 13 January 2026
Revised: 13 March 2026
Accepted: 24 March 2026
Available online: 10 April 2026

Keywords:
robotics networks, cooperative route planning, unmanned aerial vehicle, autonomous surface vehicle, hybrid optimization, artificial potential field, Real-Coded Genetic Algorithm, cubic smoothing spline, peer-to-peer wireless network

ABSTRACT

Cooperative route planning between Unmanned Aerial Vehicles (UAVs) and Autonomous Surface Vehicles (ASVs) has become an active research topic in robotics networks. In this study, a hybrid algorithm called RCGA–APF–CSS, based on a Real-Coded Genetic Algorithm (RCGA), an Artificial Potential Field (APF), and a Cubic Smoothing Spline (CSS), is proposed. The RCGA was first applied to provide a safe initial path. Subsequently, the route points were incorporated into the APF algorithm to make the route more reliable and safer by avoiding obstacles and reducing path length. To further improve the smoothness of the route, the path was smoothed using a Cubic Smoothing Spline (CSS). RCGA, APF, and RCGA–APF–CSS algorithms were applied in a hybrid 2D/3D environment of 300 × 300 × 30 m. In the first stage, the UAV uses route-finding to search for the target. Simulation results indicate that, compared with the RCGA and APF algorithms, the proposed method reduces the route length by 7.22% and 10.87%, respectively, and reduces the number of iterations by 44.4% and 33.3%, respectively. The target coordinates were sent to the ASV via a peer-to-peer wireless network. In the second stage, the ASV plans a route to the received target location; the proposed method reduces route length by 8.06% and 11.9% relative to RCGA and APF, respectively, and reduces the number of iterations by 44.4% and 33.3%. To prove the efficiency of the proposed algorithm, previously reported methods were compared with it. Compared with a polynomial-function–based planner reported for a 3D environment, the proposed method improves route length by 27.55%. In a second comparison against the ABC–SPPSO hybrid method in a 2D environment, the proposed method improves route length and maximum iterations by 10.29% and 9.09%, respectively. Overall, the proposed RCGA–APF–CSS hybrid model improves cooperative route planning for UAV–ASV coordination in complex workspaces.

1. INTRODUCTION

Unmanned Aerial Vehicles (UAVs) and Autonomous Surface Vehicles (ASVs) are combined in a robotics network to create a framework for a smart and scalable cooperative system. UAVs are becoming increasingly environmentally conscious due to their aerial sensing capabilities, but ASVs can be used to perform tasks and move on the surface. Various agents will share information, enabling real-time route planning optimization, obstacle collision avoidance, and task optimization. This allows the very difficult missions, like maritime surveillance and Search and Rescue (SAR), to be very successful [1]. In the mainstream of theoretical prototypes in this field, agent-based communication, distributed optimization, and robust decision-making strategies are included. One aspect of robotics under focus is Multi-Robot Systems (MRSs), which offer benefits over single-robot systems in terms of system-wide performance, resilience, dependability, scalability, and cost. Multi-robot applications in agriculture, mining, disaster relief, space exploration, logistics, and warehouses have great benefits with multi-robots [1]. The oceanic workspace environment poses some challenges to the SAR processes in terms of its dynamic nature and limited time to coordinate and act promptly. Partnership with different rescue automatons, which are AUVs, UAVs, and Unmanned Surface Vehicles (USVs), is a main to effective showing of surveys and emergency response. These robots have the capacity to search designated regions simultaneously, providing important information in aerial, surface, and underwater views [2]. The purpose of using multiple AUV systems, which have the aim of efficiently and accurately discovering the goal from sonar images taken by Side-Scan Sonar (SSS) mounted on the AUVs, is to converge the Multi-Robot Coverage Path Planning (MCPP) problem for maritime SAR missions. Taking into account the particulars of actual maritime SAR projects [3]. It has been demonstrated that UAVs and ASVs working together can be effective in performing several tasks, specifically in environmental monitoring applications, e.g., the characterization of the very dynamic coastal areas and oil spill control [4]. Route planning,

which is one of the fundamental tasks in robotics, involves coming up with the most efficient route given a starting point and a target point to go to, free navigation [5].

Therefore, the previous few years have witnessed numerous research studies on route planning algorithms of UAVs and ASVs. Garberoglio et al. [6] suggested a MRS for an autonomous flying vehicle that captures aerial photos, which an autonomous sea vehicle can apply to evade obstacles. Through the coordination of their movements, the two robots increase the range of detection and allow adjusting the horizon of obstacle finding. The key limitation of this work is represented by relying solely on the camera, which may be due to poor lighting. Moreover, Woo et al. [7] provided the algorithms and system formations of ASV obstacle avoidance and target search tasks. The drawback of the experimental workspace is only obstacle avoidance without target exploration. It also uses LIDAR and monocular sight to find floating obstacles and totems, determining their color by the imagery from the camera. Furthermore, D'Amato et al. [8] used the Essential Visibility Graph (EVG), an optimal route plan of ASVs, and a real-time free collision avoidance algorithm to enhance a minimum cost piecewise linear route planning optimization. The disadvantage of this work is the difficulty in dealing with rapid changes in the dynamics of the workspace. In addition, Zhang et al. [9] provided a realistic solution to visual navigation and landing control of a UAV on a moving ASV whose speed is unknown. The landing process is divided into two parts, which contain GPS horizontal tracking, visual vertical, and horizontal control. The limitation of the system is represented in its complete reliance on vision and, therefore, high sensitivity to lighting and weather conditions. In this context, Erfianto et al. [10] suggested that an Autonomous Raft Vehicle (ARV) was for underwater surveys; using the A* algorithm over many waypoints could increase ARV navigation when there are obstacles along the fixed trajectory. The disadvantage of the system is that the A* algorithm may be slow in large or dynamic environments. To the corresponding route planning of heterogeneous in Autonomous Marine Vehicles (AMVs) and Autonomous Underwater Glider (AUG). Zhang et al. [11] proposed a hybrid metaheuristic approach that manages to strike a balance between global and local search of the route by fusing the Grey Wolf Optimizer (GWO) and the Equilibrium Optimizer (EO) in the context of route planning in the underwater setting. The disadvantage of this technique is that it is still susceptible to dropping into local minima, but to a lesser extent. Moreover, the addressing model of route planning of semi-autonomous unmanned vehicles. Bella et al. [12] proposed a combined cooperative scheme of a UAV to monitor and patrol the ocean area and clean the polluted area with the support of swarm USVs. The route planning issues, according to the suggested Genetic Algorithm (GA), the limitation of GA does not guarantee finding the optimal solution, only an approximation, and may fall into a local optimum or require a long time to converge. Furthermore, Zhang et al. [13] suggested the GA-based extended state observer (GAESO) to estimate external disturbances and dynamics. In addition, Zhu et al. [14] and Li et al. [15] proposed a route planning algorithm based on GA. On the other side, the modified Khatib's potential field algorithm was proposed by Iswanto et al. [16] and applied to the quadrotor. Also, Lin et al. [17] proposed an enhanced Artificial Potential Field (APF) algorithm with Bug2 algorithm for dynamical obstacle environmental avoidance of mobile robots that will remove the oscillating patterns in the route and will avoid the failure in case of facing a complex obstacle, but the disadvantage of used APF is that it is known to suffer from local minima in some environments, and Bug2 works well with simple obstacles but may become less effective with irregular or fast-moving obstacles. As well as Lee et al. [18] developed a virtual hill algorithm in order to minimize the errors throughout the choice of the driving direction and improve the effectiveness of the motion of the robots. A dead-end algorithm is also proposed in the local minimum area, which allows the robot to revert to the point where it is without going down a dead end. In addition to this, Peng et al. [19] proposed a simplified manner of resolving the local minimum problem by structuring subharmonic potential fields. Moreover, the proposed circular sampling technique ensures that the robot maintains a minimum hazard distance from obstacles, and the potential field is actually subharmonic. To resolve the problem of route planning of robotics, a combined algorithm was presented by Wu et al. [20], which integrates the APF algorithm and the IRRT* algorithm. The virtual force field of APF was then added to the search tree expansion stage of the Informed Rapidly exploring Random Trees IRRT* algorithm, and this helped a lot in the supervision of the suggested algorithm and significantly decreased extended nodes and further minimized the route length and the search time. The combination of the Artificial Bee Colony and the Self-Perception Particle Swarm Optimization was proposed by Hussein et al. [21]. This technique was used to learn the greatest course of action in a stuffy environment. Similarly, present accompanied path planning techniques mix the Ant Colony Optimizer, the Whale Optimizer, the APF, and a random jump technique. The relation between potential classical and quantum-inspired mutation funding and complementary global exploration, local optimization, smooth route generation, and the derivations of this hybrid integration, which was conducted by Yuan et al. [22]. Sang et al. [23] designed a deterministic system called Multiple Sub-Target Artificial Potential Field (MTAPF), which is based on enhanced APF. The MTAPF is a local route planning method, which refers to the global optimal route produced by a developed heuristic algorithm, and uses this optimal route to divide it into multiple sub-target nodes to form a sub-target node sequence. Moreover, Shihab et al. [24] suggested polynomial functions for routing planning and obstacle avoidance. Shabalin and Stanovov [25] studied the application of neural networks that were optimized using the Real-Coded Genetic Algorithm (RCGA) in a simulation model. Optimization of the weights and biases of the neural network makes the vehicle route smoother, more stable, and less swerving. The results illustrate that such an approach yields a very reliable enactment that is comparable to human vehicle control. Also, Wojcik and Ciszkiewicz [26] proposed the level of effectiveness with which an RCGA takes into account the perception of control locations to plan several robot routes. RCGA generates more efficient paths by making better selections of control points in the route to decrease the number of robot collisions. It has been presented that the quality of routes in terms of distance, smoothness, and robot-to-robot free navigation in the complex environment has been significantly enhanced, as per the findings. However, the limitation of this work may not work in a complex environment.

This study looks into the problem definition through two aspects. Firstly, there is difficulty in cooperation between UAV and ASV in route finding and planning due to the

complex environments they operate in. Secondly, route finding and planning with minimum distance and maximum smoothness is obstacle avoidance done between the start point and the target point.

The main contribution of this study is enhancing the collaborative robotics network route finding and planning system between the UAV and ASV, whereby the UAV conducts reconnaissance, detects the target, and sends its coordinates to the ASV using a peer-to-peer wireless network, which subsequently reaches the target via an optimized route using the proposed hybrid algorithm known as RCGA–APF–CSS route finding and planning.

This paper is organized as follows: Section 2 illuminates the UAV and ASV mathematical models. Section 3 demonstrates the research methods used in route planning algorithms. Section 4 shows the proposed system (target detection). Section 5 discusses the simulation results, and the conclusions are given in Section 6.

2. UNMANNED AERIAL VEHICLES AND AUTONOMOUS SURFACE VEHICLES MATHEMATICAL MODELS

Generally, a UAV has four rotors that are installed proportionally to provide four forces to the UAV to fly. Therefore, the UAV consists of a plane with four rotors of equivalent structure and radius and two arms. The four rotors are fixed on the four corners of the cross in a similar proportion in positions of height as shown in Figure 1 [27].

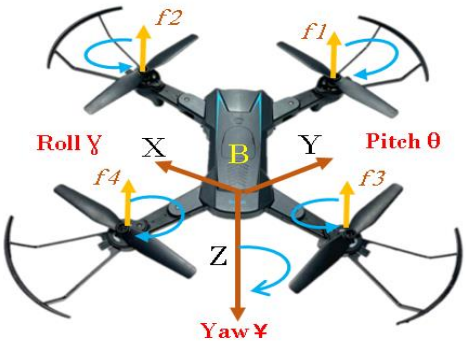

Figure 1. The scheme of the Unmanned Aerial Vehicle (UAV) model

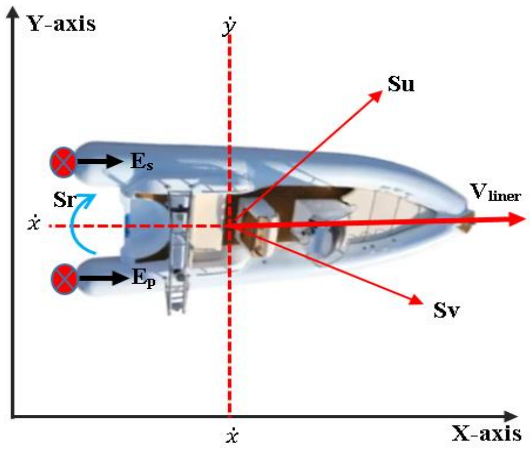

Figure 2. The scheme of the Autonomous Surface Vehicle (ASV) model

The former is B, which denotes the UAV body coordinate, and G, which denotes the ground coordinate. Thus, the altitude (x, y, and z) of UAVs' movement is related to the movement of the center of mass, and also the attitude (γ, θ, and ¥) of the UAVs' movement is related to the movement of the center of mass. Thus, the UAV model may be expressed in 6 DOF in space. Rotation of these four rotors is achieved in the following way: two rotors must rotate in an anticlockwise way (rotor 1 and rotor 3), and rotor 2 and rotor 4 have to rotate in a clockwise way. External mechanisms of the UAV, including the flight controller device and battery, are installed halfway on the body of the UAV. Elevating the UAV to flight is done by controlling the attitude and position of the UAV by varying the four rotor speeds to vary the four thrust forces, giving the formula: The lift axis of the UAV on the z-axis is determined when the four thrust forces are different [27]. To adjust the lunge force of (f_1, f_3), one moves the UAV along the x-axis, which results in a change in the pitch angle of the UAV (θ). Upon changing the lunge force of (f_2, f_4), the UAV is moved along the y-axis, and this results in a change in the roll angle (γ) of the UAV. Growing the lunge force of (f_1, f_3) and decreasing the lunge force of (f_2, f_4) allows the aerodynamic torque result to cause a yawing moment (ψ), causing the UAV to rotate around the z-axis. The state of the mathematical model that interprets the air drag of the dynamic UAV model is obtained in the study [26] as shadows:

$$\ddot{x} = (Cos\gamma\ Sin\theta\ Cos\psi + Sin\gamma\ Sin\psi)U_1 \quad (1)$$

$$\ddot{x} = (Cos\gamma\ Sin\theta\ Cos\psi + Sin\gamma\ Sin\psi)U_1 \quad (2)$$

$$\ddot{z} = (Cos\gamma\ Cos\theta)U_1 - g \quad (3)$$

$$\ddot{\gamma} = [(I_y - I_z)\dot{\theta}\dot{\gamma} - (J_r\Omega_r)\dot{\theta} + U_2]\frac{1}{I_x} \quad (4)$$

$$\ddot{\theta} = [(I_z - I_x)\dot{\gamma}\dot{\psi} + (J_r\Omega_r)\dot{\gamma} + U_3]\frac{1}{I_y} \quad (5)$$

$$\ddot{\psi} = [(I_x - I_y)\dot{\theta}\dot{\gamma} + U_4]\frac{1}{I_z} \quad (6)$$

$$\Omega_r = (w_1 - w_2 + w_3 - w_4) \quad (7)$$

$$U_1 = (f_1 + f_2 + f_3 + f_4)\frac{B}{M} \quad (8)$$

$$U_2 = l(-f_1 - f_2 + f_3 + f_4)\frac{B}{I_x} \quad (9)$$

$$U_3 = l(-f_1 + f_2 + f_3 - f_4)\frac{B}{I_y} \quad (10)$$

$$U_4 = d(f_1 + f_2 + f_3 + f_4)\frac{1}{I_z} \quad (11)$$

where, $(\ddot{x},\ddot{y},\ddot{z})$ indicate the acceleration of the UAV in the inertial frame; $(\ddot{\theta}, \ddot{\gamma}, \ddot{\psi})$ indicate the angular acceleration (roll, pitch, and yaw); and $(\dot{\theta},\dot{\gamma},\dot{\psi})$ represent the angular velocity, respectively. *C* and *S* indicate cos and sin, respectively. $f_{(1,2,3,4)}$ represents the lunge forces created by the four rotors that may be watched as control signals to the UAV system. The UAV arm length, the UAV mass, and the coefficient of lunge are denoted by l, M, and B, respectively. Moreover, the A marine ASV is a type of smart autonomous marine robot

that has the benefits of intelligent and flexible applications. Naval ASVs play a main role in naval research, marine commerce, environmental preservation, and national security. The ASV with two control inputs and three degrees of freedom, the structure of the ASV is shown in Figure 2 [28].

The ASV has two high-capacity ducted engines that provide a means of propulsion and steering of the ASV. Such an engine offers two different types of inputs, including E_s and E_p, and also the direction of the ASV (x, y, θ). Therefore, the motion equations establish an important starting point for the structure of the mathematical model of an ASV. Specifically, the equations of kinematics labelling the movement of the vehicle are the following [21]:

$$\dot{x} = S_u \ cos\ \phi - S_v \ sin\ \phi \tag{12}$$

$$\dot{y} = S_u \ sin\ \phi + S_v \ cos\ \phi \tag{13}$$

$$\dot{\phi} = S_r \tag{14}$$

The dynamic equations of the ASV motion include Eq. (15), Eq. (16), and Eq. (17) [26]:

$$m\,\dot{S_u} - m\,S_v S_r + C_u S_u = E_s + E_p \tag{15}$$

$$m\,\dot{S_v} + m\,S_u S_r + C_v S_v = 0 \tag{16}$$

$$J\,\dot{S_r} + F_r S_r = L(E_s - E_p) \tag{17}$$

The definitions of physical ASV parameters of Eq. (12) to Eq. (17) are taken from the study [21], as displayed in Table 1.

Table 1. Autonomous Surface Vehicle (ASV) physical parameters definitions

Parameter	Definition
S_u	Surge speed
x	coordinates to the centre of mass
ϕ	Vehicle's orientation
M	Vehicle's mass
C_v	Coefficient viscous
E_s	Left engine force
L	Arm of the forces
S_v	Sway speed
y	Coordinates to the centre of mass
S_r	Speed angular
J	Inertia rotational
F_r	Friction rotational
E_p	Right engine force

3. RESEARCH METHODS USED IN ROUTE PLANNING ALGORITHMS

This section presents the investigation methods of the route planning algorithms that were used in our proposed algorithm, RCGA–APF–CSS.

3.1 Real-Coded Genetic Algorithm

RCGA is a modernized version of the classical GA, in the chromosome representation, where binary coding is substituted with direct encoding based on the real-valued domain. This, in a way, makes the whole process easier and quicker as there are no encoding transformations and decoding, thus resulting in faster convergence, particularly in problems related to continuous optimization [29]. The RCGA is significantly applicable to the field of robotic, UAVs, and AUVs path planning since it can depict path points, angles, elevations, and speeds as real-world variables. This leads to the creation of paths that are not only smooth but short and safe by the system's dynamic constraints, with the consideration of obstacles. RCGA is used as an optimization for finding an answer to a problem by creating a random population of possible solutions [30]. As mentioned earlier, the RCGA is working on real values as shown by the three key expressions.

$$X = [x_1 + x_2 + \cdots + x_n] \tag{18}$$

where, X denotes the chromosome representation, $x_i \in \mathbb{R}$ represents gene number i in the RCGA algorithm, it represents a real variable. Then the arithmetic crossover is achieved according to the following expression:

$$X_{cr} = \varphi X_a + (1 - \varphi)\, X_b \tag{19}$$

where, X_{cr} is the recently generated chromosome, φ is the real mixing coefficient, X_a, X_b are the first and second parent chromosomes, respectively.

The mutation of RCGA real-valued is completed in the following way:

$$x_i' = x_i + \mathcal{N}(0, \rho^2) \tag{20}$$

where, x_i' is the gene after mutation, x_i represents the Gene value before mutation. Gaussian distribution with zero mean and variance ρ^2.

In addition, the application of route planning and the cost of energy needed to operate each route are used as the main criteria. Then, more possible solutions to the problem (offspring) are formed by using a procedure known as crossover, which combines the best and finest solutions obtained in the previous generation of parents. Moreover, alternative mutations of the most suitable solutions are generated during the mutation procedure. Then, the RCGA re-runs the selection with the successive potential solutions of the population that are even closer and closer to the right solution until a certain end condition, say, the number of generations, is met [31]. The main strength of the RCGA technique is that there is a chance of quick and universal stochastic. looking for the best possible solutions. Furthermore, the algorithm is simple to apply and can be employed to address complex issues, e.g., to find the optimal route of the AUV, ASV at the underwater location when there are both static and dynamic obstacles. The algorithm decreases the risk of the local minima problem because searching for the best solutions is random. As a whole, the technique does not need to have huge amounts of computations to resolve the route planning topic. Furthermore, the route can be inefficient in case of an inadequate number of generations being run. The more the generations, the narrower the route develops [30]. To obtain the best cost function, the worst solutions are always taken out of the population. This applies to a fast-changing or very complicated environment, where it takes a lot more work to find a solution [31]. The RCGA algorithm in route finding and planning is presented in the following steps:

Step 1: Start the initial population route.

Step 2: Calculate fitness value.

Step 3: Check the collision obstacle. Otherwise, go back to Step 2.

Step 4: Apply selection, crossover, and mutation using the actual values.

Step 5: Check stopping condition. the best fitness value (route distance, smoothness). Otherwise, back to step 2.

Step 6: Generate route, end.

3.2 Artificial Potential Field algorithm

The APF method originated in 1986, and it includes the assumption that there is a revolting field surrounding the obstacle and a striking area surrounding the goal in which a stirring vehicle (e.g., AUV, ASV). Because of the interplay of such virtual fields, the force that is produced is premeditated in reference to the direction the vehicle is traveling. Through this approach, there is no need to have previous knowledge of the workspace environment and where the obstacles are detected [32]. Moreover, applied irrespective of whether the obstacles in the workspace environment that the AUV, ASV is traveling in are persistently moving, or not, and whether they are smooth or unbalanced. The most important condition in this algorithm to make it efficient is the correct detection of obstacles. The benefit of the APF approach is that it is simple and easy to implement, and does not require many calculations, which allows one to control AUVs and prevent free collisions in close to real time. Though the abovementioned benefits are various, there is a chance of local minima or trap situations that are viewed as a main drawback [30]. Moreover, there are conditions under which, as in the case of a U-shaped barrier, the resulting force on the AUV/ASV will be composed such that the algorithm will cause the movement of the AUV/ASV in an infinite loop without reaching the target [30]. The APF algorithm in route finding and planning is introduced in the following steps:

Step 1: Start with the initial value (map, star, and target node)

Step 2: Calculate the attractive potential.

Step 3: Calculate the repulsive potential.

Step 4: Calculate the total potential.

Step 5: Calculate the vector force.

Step 6: Update position.

Step 7: If the target is reached. Otherwise, go back to Step 5.

Step 8: Generate the route.

3.3 Cubic Smoothing Spline

In general, the Cubic Smoothing Spline (CSS) is the mathematical model that can be used to create a curve smoothly through several nodes. The cubic spline interpolation is an irregular technique that gives a constant line of a collection of interpolation nodes via cubic polynomials. The close-fitting cubic spline interpolation route planning of the robot is smoother, and this provides the robot with further dynamic physical characteristics in an emergency break or emergency steering, which provides it with immense benefits compared to a route that includes straight lines and arcs. Then, the definition of cubic spline interpolation and the technique of generating the route will be presented [33]. The steps of the CSS are as follows:

Step 1: Start to input the node route.

Step 2: Defined the object function (smoothness).

Step 3: Choose the smooth coefficient.

Step 4: Deriving the linear system.

Step 5: Construct and evaluate the route.

The CSS $s(x)$ is obtained to minimize the following function:

$$s(x) = \sum_{i+1}^{n} (y_i - s(x_i))^2 + \lambda \int_a^b [(\ddot{s}\,(x)]^2 dx \qquad (21)$$

where, y_i is the observed data, x_i is data input, $(y_i - s(x_i))^2$ is the fitting squared error, $\ddot{s}(x)$ is the second derivative of $s(x)$, $\int_a^b [(\ddot{s}\,(x)]^2 dx$ is a penalty smoothness term, and λ is the smoothing parameter.

4. PROPOSED SYSTEM (TARGET DETECTION)

This section demonstrated the proposed system of cooperation based on route finding and planning target detection for UAV and ASV. Figure 3 shows the proposed system, which first applies the route-finding algorithm (RCGA–APF–CSS) in the UAV to detect the target and then sends the node target (x, y) through the Wi-Fi connection (peer-to-peer wireless network) to the ASV. Also, the route-planning algorithm (RCGA–APF–CSS) was applied in ASV.

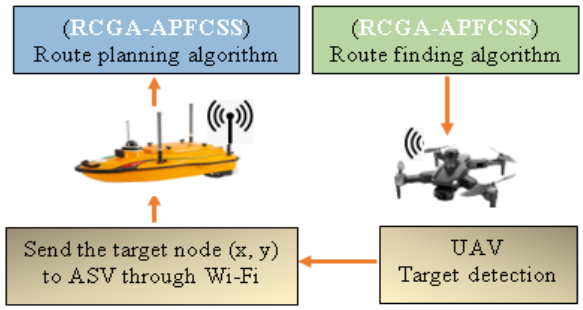

Figure 3. The proposed system for target detection

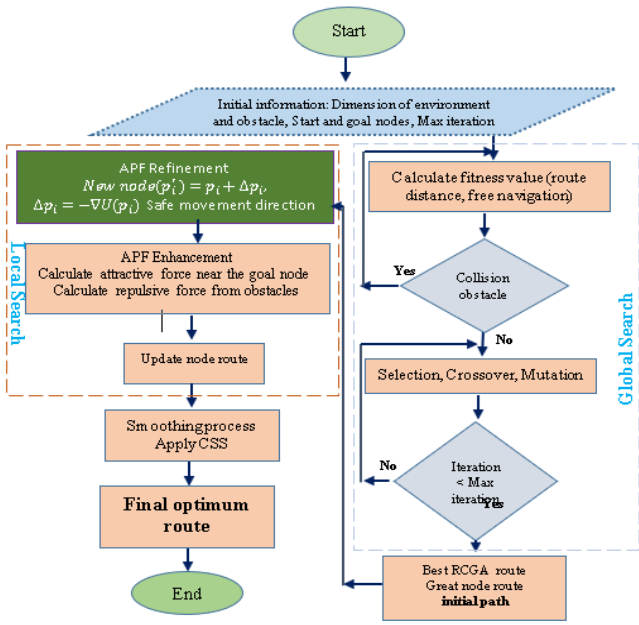

Figure 4. Flow chart of the proposed (RCGA–APF–CSS) route finding and planning algorithm

Note: RCGA: Real-Coded Genetic Algorithm; APF: Artificial Potential Field; CSS: Cubic Smoothing Spline.

Moreover, the proposed approach to route finding and planning mixes two algorithms, RCGA and APF, and consequently, smooths the route using CSS. Combining the two will develop a hybrid algorithm called RCGA–APF–CSS. Figure 4 is a flowchart that explains the RCGA–APF–CSS proposed algorithm. Mainly, the RCGA algorithm was used to find a route that avoids collisions. It works by guiding the route finding and planning of UAV and ASV from the starting node to the goal node. Moreover, it moves from node to node while steering clear of obstacles until it reaches the destination. Nevertheless, RCGA doesn't frequently find the optimum route. It habitually makes a winding route that ends up consuming more power and covering extra distance. Subsequently, the candidate nodes identified by RCGA were used for further processing. Secondly, the candidate nodes found using RCGA were fed into the APF algorithm.

The APF refinement depends on the following equation:

$$p'_{ni} = p_{oi} + \Delta p_{oi} \tag{22}$$

$$\Delta p_{oi} = -\nabla U(po_i) \tag{23}$$

where, p'_{ni} is the node of new path, p_{oi} is the node of initial path, Δ is the direction of the path to avoid the obstacle, and $U(po_i)$ is the potential field between the obstacle and the target. Moreover, APF helped create the shortest route and then used CSS to produce the smoothest and shortest route.

An illustration of a heuristic distance metric that is employed by the route planning algorithm is the Euclidean distance for a 3D and 2D coordinate system used as shown below [27]:

$$3Dis_{route=}\sqrt{\begin{matrix}(x_o - x_n)^2 + (y_o - y_n)^2 \\ +(z_o - z_n)^2\end{matrix}} \tag{24}$$

$$2Dis_{route=}\sqrt{(x_o - x_n)^2 + (y_o - y_n)^2} \tag{25}$$

5. SIMULATION RESULTS

This research used the RCGA, APF, and proposed algorithm RCGA-APF–CSS, and implementation setups in 3D UAV and 2D ASV in an environment of 300 × 300 × 30 m. Intel Core i7 tenth-generation computer hardware, which includes a 1.7 GHz CPU and 16.00 GB RAM in addition to the MATLAB 2024b package, was used. There are three algorithms, namely the RCGA algorithm and the APF algorithm, and the proposed hybrid RCGA–APF–CSS algorithm, which apply to route finding in UAV to detect the target and then apply to route planning in ASV, which determines a collision-free route, and the results of the algorithms are compared between them to find the shortest distance route, bearing in mind that there has to be a safety zone between the obstacles and the robotics. The location of the start node of the UAV is at 21, 21, 22 m, and the location of the target node is at 280, 240, 0 m. After applying the RCGA, using Eq. (19), the distance of the optimal route was equal to 423.3 m in max iteration number 90, as demonstrated in Figure 5. On the other hand, the ASV optimal distance of the route by used the Eq. (20) equal to 420.2 m in max iteration number 90 is presented on Figure 6 in case the RCGA algorithm was applied to the proposed environment were the location of the start node of the ASV is at 100, 0 m, and location of the target location at 280, 240 m.

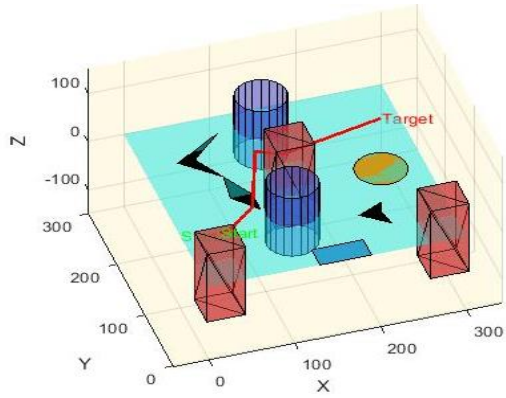

(a) The optimal route finding of the UAV

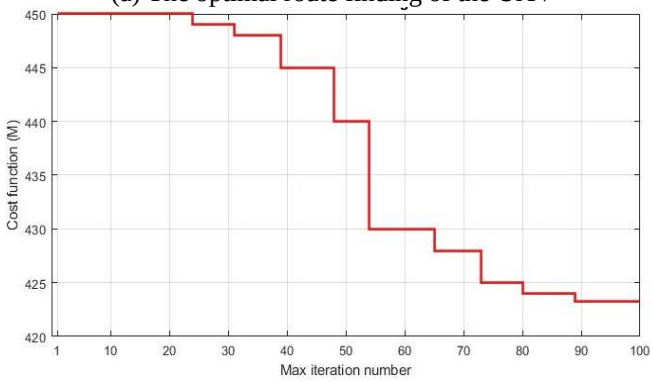

(b) The cost function

Figure 5. Simulation test result of the Real-Coded Genetic Algorithm (RCGA) algorithm

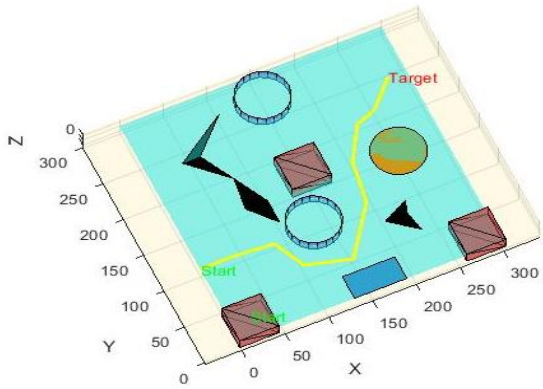

(a) The optimal route planning of an Autonomous Surface Vehicle (ASV)

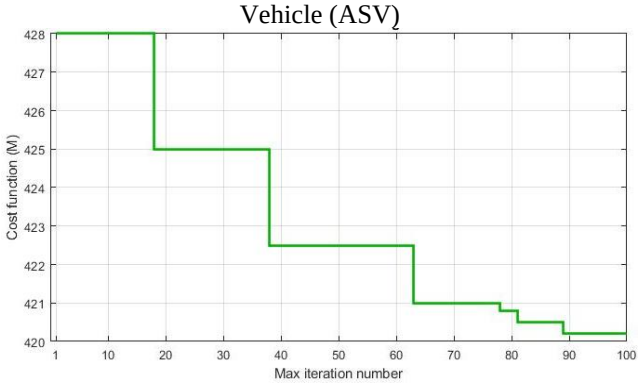

(b) The cost function

Figure 6. Simulation test result of the Real-Coded Genetic Algorithm (RCGA) algorithm

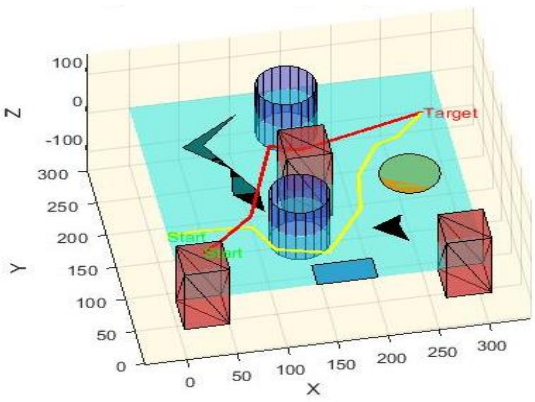

Figure 7. The Real-Coded Genetic Algorithm (RCGA) algorithm route planning of cooperation based on target detection for Unmanned Aerial Vehicle (UAV) and Autonomous Surface Vehicle (ASV)

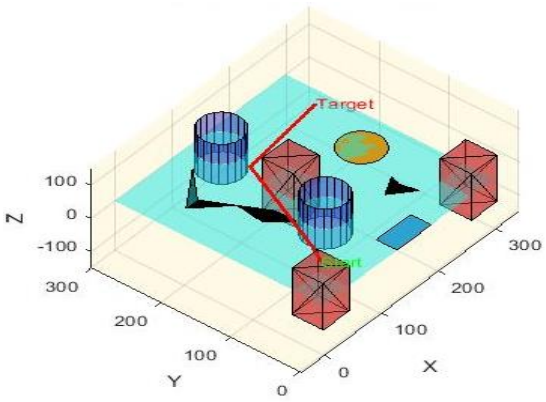

(a) The route finding of the Unmanned Aerial Vehicle (UAV)

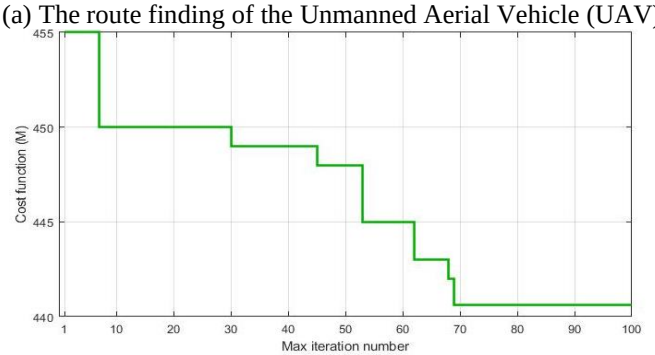

(b) The cost function

Figure 8. Simulation test result of the Artificial Potential Field (APF) algorithm

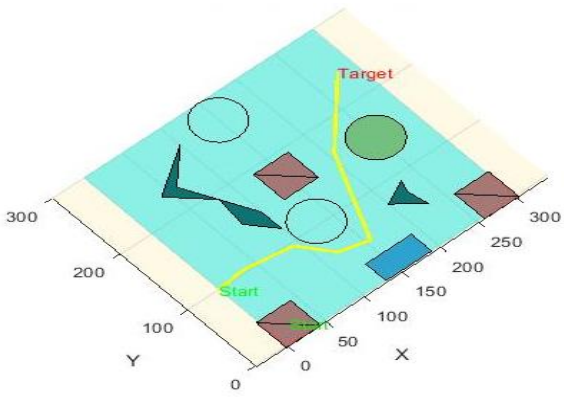

(a) The optimal route planning of an Autonomous Surface Vehicle (ASV)

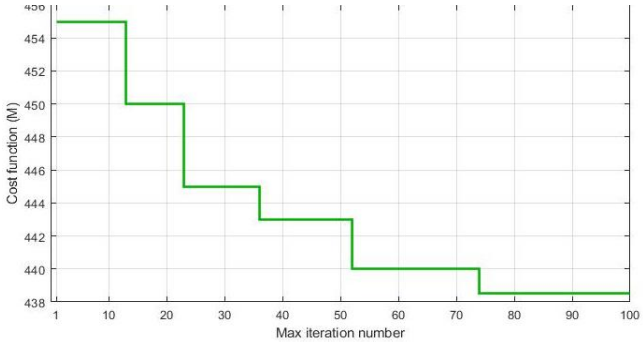

(b) The cost function

Figure 9. Simulation test result of the Artificial Potential Field (APF) algorithm

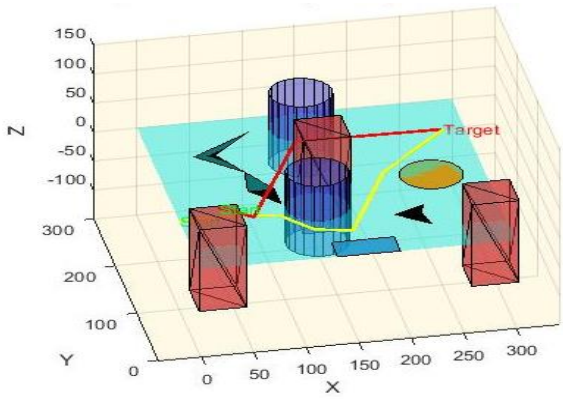

Figure 10. The Artificial Potential Field (APF) algorithm route planning of cooperation based on target detection for Unmanned Aerial Vehicle (UAV) and Autonomous Surface Vehicle (ASV)

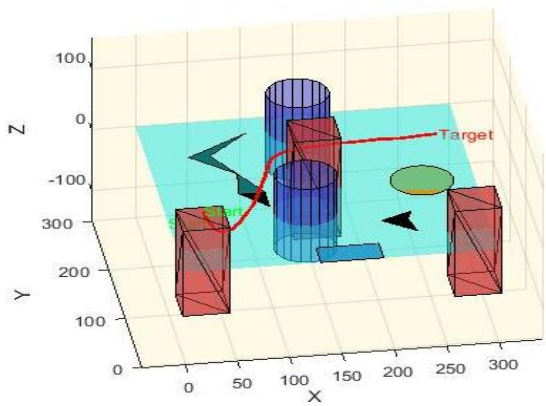

(a) The optimal route

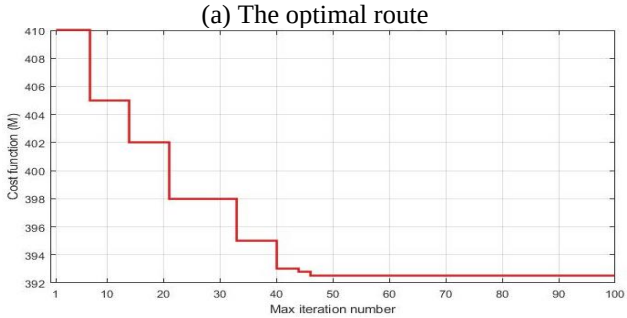

(b) The best cost function convergence

Figure 11. The proposed algorithm (RCGA–APF–CSS) in UAV

Note: RCGA: Real-Coded Genetic Algorithm; APF: Artificial Potential Field; CSS: Cubic Smoothing Spline; UAV: Unmanned Aerial Vehicle.

Figure 7 shows the RCGA algorithm route planning of cooperation based on target detection for UAV and ASV. Figure 8 shows the optimal route distance in the proposed workspace environment when the APF algorithm was applied to the UAV. The optimum cost function distance is 440.6 m, which was observed in the maximum iteration number of 75. Moreover, Figure 9 shows the optimal route distance in the proposed workspace environment; when the APF algorithm was applied in ASV, the cost function of the route is 438.5 in the maximum iteration 75.

Moreover, Figure 10 illustrates the APF algorithm route finding and planning of cooperation based on target detection for UAV and ASV. In addition, in Figure 11(a), the RCGA–APF–CSS hybrid algorithm was proposed to identify the optimal route in the same proposed workspace environment applied to a UAV. The optimal path distances will have a value of 392.7 m. The best cost function convergence was discovered with the optimum number of 50 iterations, as represented by Figure 11(b).

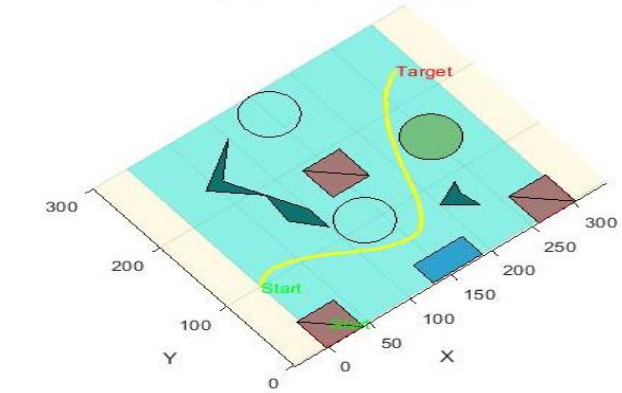

(a) The optimal route

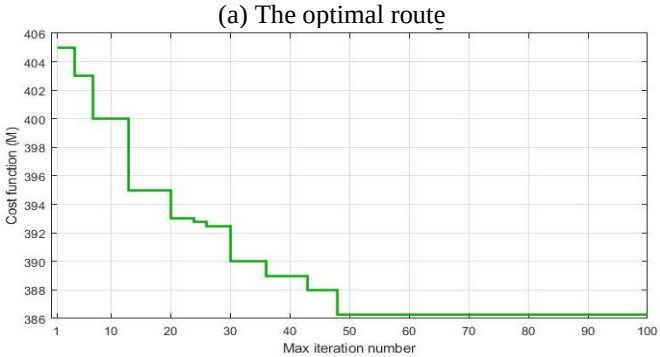

(b) The best cost function convergence

Figure 12. The proposed algorithm (RCGA–APF–CSS) in ASV

Note: RCGA: Real-Coded Genetic Algorithm; APF: Artificial Potential Field; CSS: Cubic Smoothing Spline; ASV: Autonomous Surface Vehicle.

Moreover, Figure 12(a) proposes the use of the RCGA–APF–CSS hybrid algorithm that aims at finding the best route within the same suggested environment that is implemented in ASV. The optimal route distance determination takes a value of 386.3 m. The optimum number of max iterations of 50 iterations was created to be the best cost convergence function, as illustrated by Figure 12(b). Furthermore, Figure 13 demonstrates the (RCGA–APF–CSS) proposed algorithm route planning of cooperation based on target detection for UAV and ASV.

In addition, the speed of the UAV and ASV corresponds to the route finding and planning distance, as shown in Figure 14. Moreover, the UAV acceleration profile is shown in Figure 15. This is resulting from the speed, which is the difference between two points, and also shows where the UAV is accelerating or decelerating.

Moreover, Figure 16 illustrates the elevation gradient UAV is deduced from the height and distance, which demonstrates the slope of the path up/down (dz/ds). Additionally, Figure 17 shows the curvature of the UAV. It will result from the (x, y, z) coordinates, which measure the intensity of the bending and curvature of the UAV.

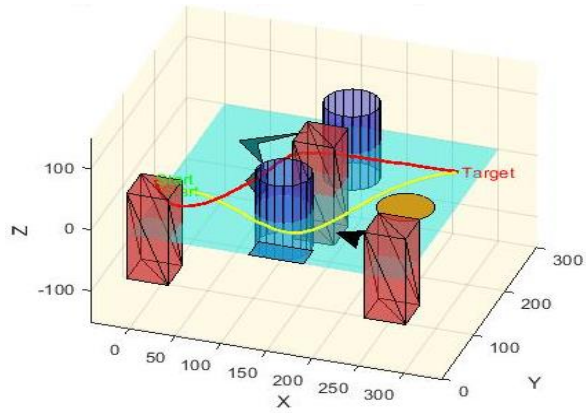

Figure 13. The RCGA–APF–CSS proposed algorithm route planning of cooperation based on target detection for UAV and ASV

Note: RCGA: Real-Coded Genetic Algorithm; APF: Artificial Potential Field; CSS: Cubic Smoothing Spline; UAV: Unmanned Aerial Vehicle; ASV: Autonomous Surface Vehicle.

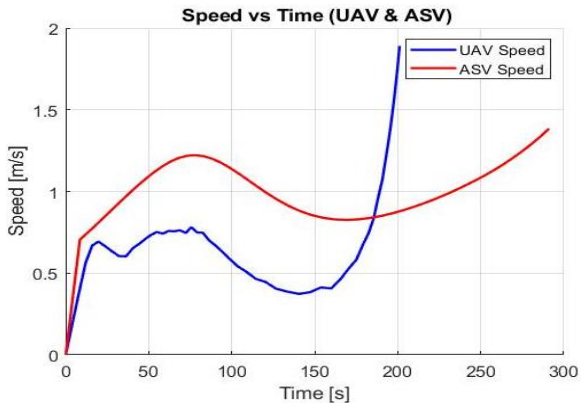

Figure 14. The speed of Unmanned Aerial Vehicle (UAV) and Autonomous Surface Vehicle (ASV)

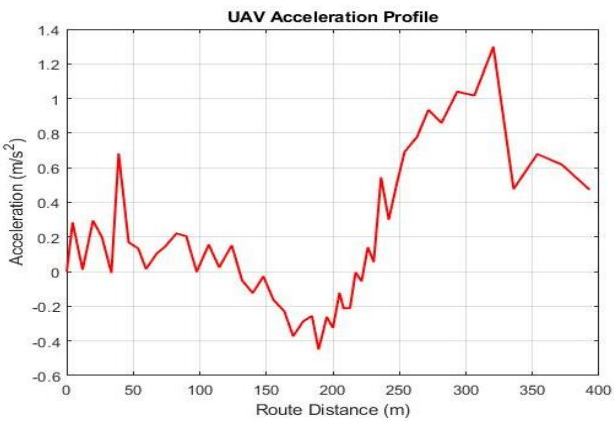

Figure 15. The Unmanned Aerial Vehicle (UAV) acceleration profile

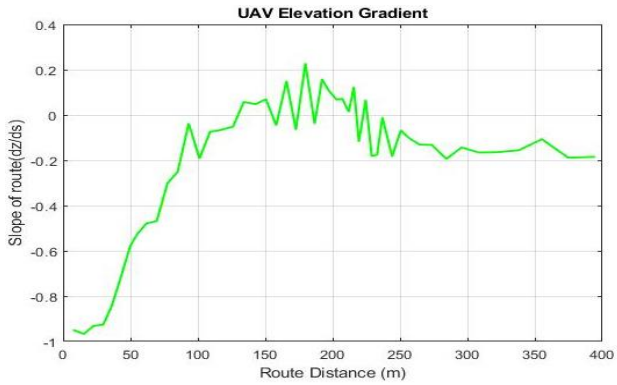

Figure 16. The elevation gradient

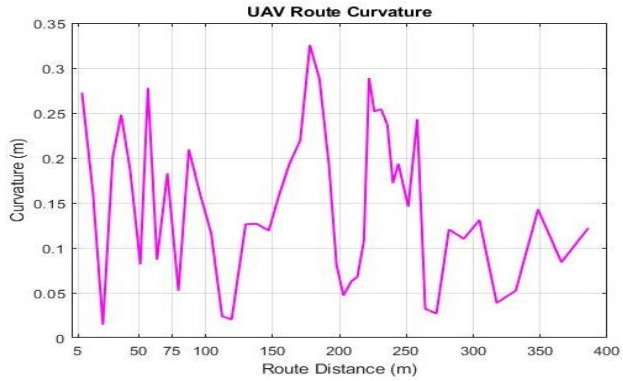

Figure 17. The curvature of an Unmanned Aerial Vehicle (UAV)

Through the comparison of the RCGA and APF with the proposed hybrid algorithm RCGA–APF–CSS, it has been realized that the proposed algorithm produced the shortest route between the starting node and the target node, as shown in Table 2.

Table 2. Comparison of the optimal route finding and planning distance

Algorithm	Route Length (m)		No. of Iteration
	UAV	ASV	
RCGA	423.3	420.2	90
APF	440.6	438.5	75
Proposed RCGA–APF–CSS	392.7	386.3	50

Note: RCGA: Real-Coded Genetic Algorithm; APF: Artificial Potential Field; CSS: Cubic Smoothing Spline; UAV: Unmanned Aerial Vehicle; ASV: Autonomous Surface Vehicle.

Also, a safety zone represents the minimum distance between the UAV, ASV, and the obstacle, as shown in Eq. (26) [33].

$$Ds_m = \| p_n - c_o \| - r_o \tag{26}$$

where, Ds_i is the distance between the path node p_n and obstacle, $\| \|$ is the Euclidean distance, Ds_{m} is the min distance, c_o is the center of the obstacle, and r_o is the obstacle radius. In addition, the smoothness route (turning angle) is shown in the following equations [33]:

$$v_n = p_n - p_{n-1} \tag{27}$$

$$\theta_n = \cos^{-1}\left(\frac{v_n \cdot v_{n+1}}{\| v_n \| \| v_{n+1} \|}\right) \tag{28}$$

$$S_m = \sum_{n=2}^{n-1} \theta_n \tag{29}$$

where, v_n is the motion vector for node route, θ_n is the turning angle of the node route, $(\cdot)$ is the dot product, and S_m is the smoothness route. Finally, the execution time in algorithms can be seen in Eq. (30):

$$T_c = T_{end} - T_{start} \tag{30}$$

Table 3 presents the safety zone distance, route smoothness (turning angle), and execution time for all implementation algorithms.

Table 3. The safety zone distance, route smoothness (turning angle), and execution time

Algorithm	Safety Zone Distance (m)		Turning Angle (rad)		Execution Time (s)	
	UAV	ASV	UAV	ASV	UAV	ASV
RCGA	1.9	1.7	3.8	3.7	0.70	0.65
APF	1.5	1.4	2.6	2.4	0.28	0.25
Proposed RCGA–APF–CSS	2.3	2.0	1.7	1.6	0.33	0.28

Note: RCGA: Real-Coded Genetic Algorithm; APF: Artificial Potential Field; CSS: Cubic Smoothing Spline; UAV: Unmanned Aerial Vehicle; ASV: Autonomous Surface Vehicle.

As well as Figure 18, the mean value distance of the route planning for all algorithms was used, where the number of attempts is 10. Moreover, the effectiveness of the route distance of the suggested algorithm E_r and the effectiveness of the iteration E_i were determined according to the following formula:

$$E_r = (1 - \frac{N_r}{O_r}) \times 100\% \tag{31}$$

$$E_i = (1 - \frac{N_i}{O_i}) \times 100\% \tag{32}$$

where, N_r is the new route, O_r is the old route, N_i is the new iteration and O_i is the old iteration. Table 4 summarizes the enhancement of route distance and iteration number compared to the proposed algorithm. Also, the best values of the parameters in the RCGA–APF–CSS algorithm are shown in Table 5.

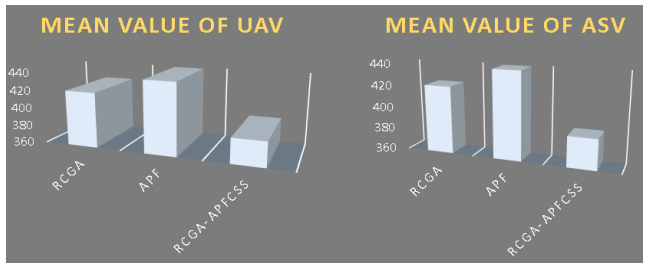

Figure 18. The mean value distance of the route finding and planning algorithms

Table 4. The enhancement of the route distance and iteration

Algorithm	E_r(%)		E_i(%)	
	UAV	ASV	UAV	ASV
RCGA	7.22	8.06	44.4	44.4
APF	10.87	11.9	33.3	33.3

Note: RCGA: Real-Coded Genetic Algorithm; APF: Artificial Potential Field; UAV: Unmanned Aerial Vehicle; ASV: Autonomous Surface Vehicle.

Table 5. Best values of the parameters in RCGA–APF–CSS

Parameter	Value
N_m	6
P_s	35
gens	80
P_c	0.85
P_m	0.2
C_{att}	1
w_{coll}	1000
C_{rep}	8
E_{dis}	3.5
alpha	0.2
tolerance	0.5
Max. Iteration	100

Note: RCGA: Real-Coded Genetic Algorithm; APF: Artificial Potential Field; CSS: Cubic Smoothing Splin.

In addition, the enhancement of the mean value (%) for the results distance in Table 2 is shown in Table 6.

Table 6. The mean value (%)

Algorithm	The Mean Value (%)	
	UAV	ASV
RCGA	99.69	99.7
APF	99.84	99.81
Proposed RCGA–APF–CSS	99.73	99.7

Note: RCGA: Real-Coded Genetic Algorithm; APF: Artificial Potential Field; CSS: Cubic Smoothing Spline; UAV: Unmanned Aerial Vehicle; ASV: Autonomous Surface Vehicle.

To compute the peer-to-peer wireless network Wi-Fi communicator mathematical formulation between the UAV and ASV, it is notable to state that these equations are approximations of the metrics of the network performance, which are dynamic and which are established on the simulation. Their concepts are attenuation, signal-to-noise ratio (SNR), reliability, packet loss, latency, throughput, and Quality of Service (QoS) [33].

$$Pl_d = 20\log_{10} d + 20\log_{10} f + C \tag{33}$$

where, Pl_d is the path loss (attenuation) with route distance in dB, d is the distance between UAV and ASV in m, f is the signal frequency in MHz, C is the conversion constant to convert the distance from m and frequency from MHz to dB [34].

$$P_r = T_P - Pl_d \tag{34}$$

$$SNR = T_p - N_p \tag{35}$$

where, R_r is the power received in dBm, T_P is transmit power in dBm, N_p is the noise power in dBm, SNR is the signal-to-noise ratio in dB [33].

$$R = 1 - e^{-SNR/10} \tag{36}$$

where, R is the readability, which represents the probability of successful packet delivery [34].

$$P_L = 1 - R \tag{37}$$

where, P_L is the packet loss.

$$L_y = t_{propagation} + t_{processing} + £ \tag{38}$$

$$t_{propagation} = \frac{d}{c} \times 10^3 \tag{39}$$

where, L_y is the latency in ms, $t_{processing}$ is the fixed processing delay, c is the speed of light, £ is a small random noise. The throughput of data is represented in Eqs. (40)-(41) [35].

$$D_{rate} = B \times \log_2 1 + SNR_{liner} \tag{40}$$

$$SNR_{liner} = 10^{SNR/10} \tag{41}$$

where, D_{rate} is the data rate, B is the bandwidth.

Therefore, Figure 19 shows the QoS of Wi-Fi peer-to-peer between UAV and ASV.

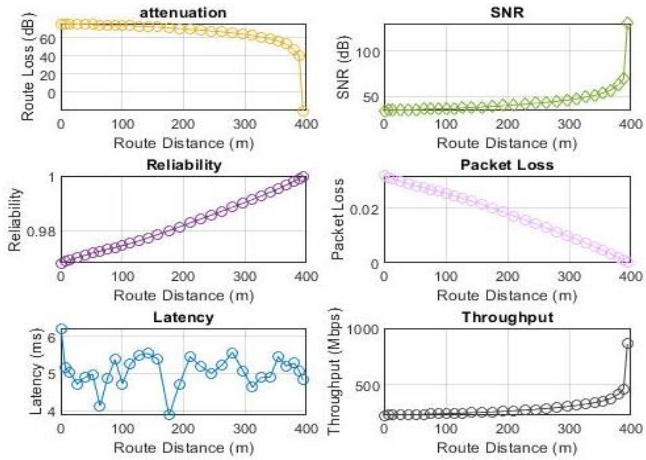

Figure 19. Quality of Service (QoS) of Wi-Fi between UAV and ASV

Note: UAV: Unmanned Aerial Vehicle; ASV: Autonomous Surface Vehicle.

To verify the efficiency of the proposed algorithm, the first algorithm comparison was done to test with RCGA, APF, and our proposed algorithm, RCGA–APF–CSS. It was compared to the study [24], which used a 3D map environment in a UAV and applied two types of polynomial functions. This algorithm was applied in a stationary workspace environment without a change in the working space, where the workspace environment is 10 × 9 × 9 m, the starting node is 1, 3.8, 2 m, and the target node is 6.5, 6.3, 2 m. Figure 20(a) demonstrates that this environment was used in RCGA, APF, and proposed algorithms to locate the most optimal route to follow by the UAV. The best route was also obtained using the RCGA-APF, RCGA–APF–CSS algorithm, and best distance cost functions in Figures 20(b) and (c), respectively.

The second comparison was carried out with the Artificial Bee Colony Self Perception Particle Swarm Optimization (ABC–SPPSO) [21]. The 2D workspace environment is 500 × 500 cm, the starting point is 50, 50 cm, and the goal point is 350, 450 cm. It is the same environment that applies to the RCGA, APF, RCGA–APF, and proposed RCGA–APF–CSS

algorithms illustrated in Figure 21(a), furthermore, Figures 21 (b) and (c) demonstrate the RCGA–APF and proposed RCGA–APF–CSS algorithm and best cost distance function, respectively.

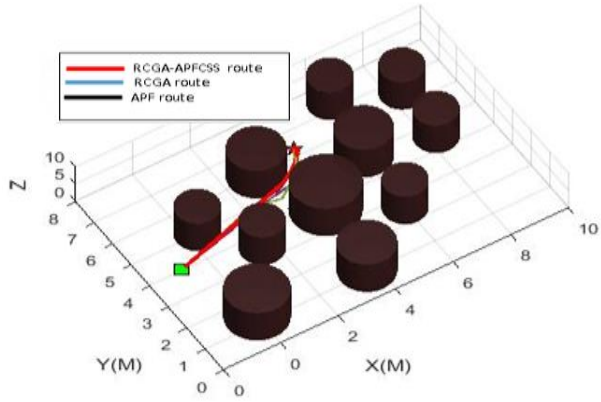

(a) 3D map using (RCGA, APF and RCGA–APF–CSS) algorithms

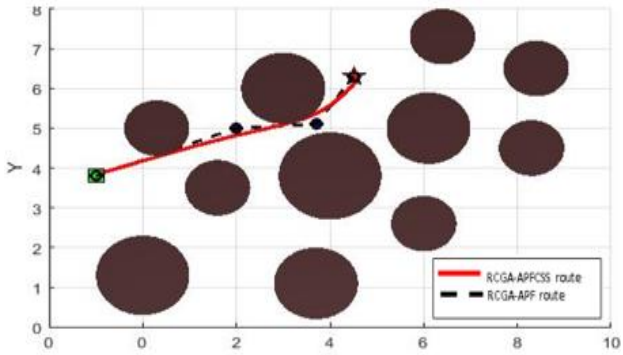

(b) 3D map using (RCGA–APF and RCGA–APF–CSS) algorithm

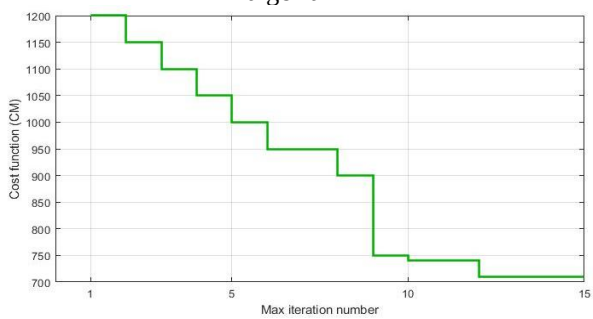

(c) The best cost distance function of the RCGA–APF–CSS algorithm

Figure 20. The simulation results using the workspace [24]
Note: RCGA: Real-Coded Genetic Algorithm; APF: Artificial Potential Field; CSS: Cubic Smoothing Spline; UAV: Unmanned Aerial Vehicle; ASV: Autonomous Surface Vehicle.

Tables 7 and 8 demonstrate that the proposed hybrid algorithm provides a route with a shorter route distance and consumes less time in finding the best route compared to the literature [21, 24]. Moreover, Table 9 shows the values of the parameters in the ABC-SPPSO algorithm in the study [21].

The reason for the superiority of the proposed hybrid algorithm is due to the use of an RCGA solution to UAV and ASV route finding and planning. Standardization, deletion, and addition of operons have been presented in the design of genetic operons to counteract the deficiency of basic operons. At the same time, RCGA is optimized using adaptive mutation and crossover rate. One way to improve the algorithm is to include new operators and dynamic ways of addressing the problem of the target node not being obtained because of the local minima during the evolution process. The nodes produced by the initial route were then injected into the algorithm APF. The APF technique is widespread and easy to solve the route planning issue. It is a distinctive methodology and has a simple computation model; thus, it is a desirable choice in real-time and dynamic settings. This method was short and obstacle-free. To achieve a smoother route, the CSS technique was used, which worked to that end.

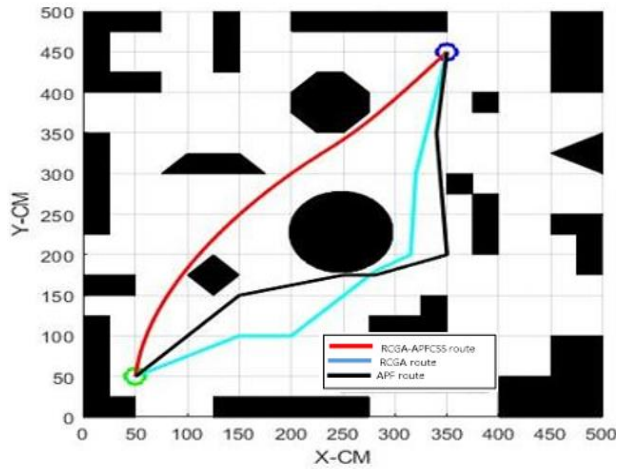

(a) Using the (RCGA, APF, and RCGA–APF–CSS) algorithms

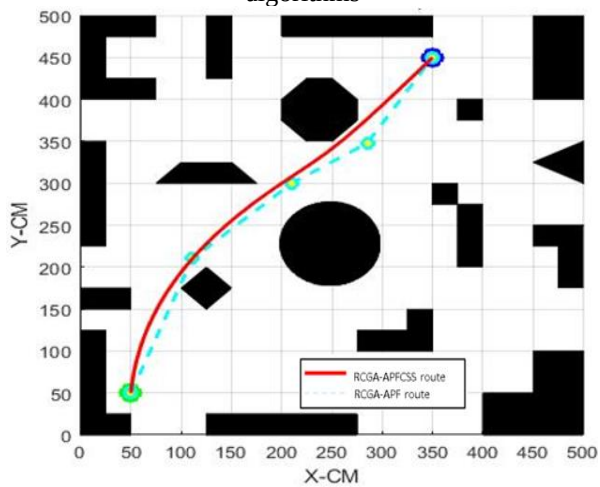

(b) Using the (RCGA–APF, RCGA–APF–CSS) algorithms

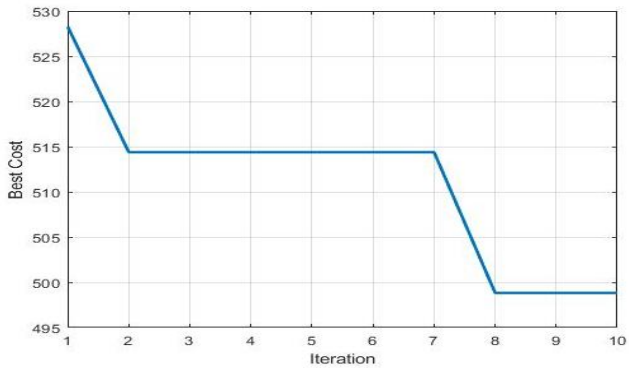

(c) The best cost distance function of the RCGA–APF–CSS algorithm

Figure 21. The test results using a 2D environment of study [21]
Note: RCGA: Real-Coded Genetic Algorithm; APF: Artificial Potential Field; CSS: Cubic Smoothing Spline; UAV: Unmanned Aerial Vehicle; ASV: Autonomous Surface Vehicle.

Table 7. The optimal route distance of the proposed algorithm compared to the study [24]

Ref.	Algorithm	Route Distance (cm)	E_r (%)	E_i (%)
[24]	Polynomial 4th	980	27.55	-
	Polynomial 5th	1.470	51.7	-
	A*	2.010	64.67	-
	RCGA	890	20.22	44.4
	APF	920	22.82	33.3
	Proposed RCGA–APF–CSS	710	-	-

Table 8. The optimal route distance of the proposed algorithm compared to the study [21]

Ref.	Algorithm	Route Distance (cm)	E_r (%)	E_i (%)
[21]	hybrid ABC-SPPSO	555.36	10.29	9.09
	RCGA	600.56	17.04	44.4
	APF	740.21	32.69	33.3
	Proposed RCGA–APF–CSS	498.13	-	-

Table 9. The values of the parameters in the Artificial Bee Colony Self Perception Particle Swarm Optimization (ABC–SPPSO) algorithm [21]

Parameters	Values
Scout Bees numbers	10
Selected Bees numbers	5
Recruit Bees numbers equal to the population size of SPPSO	40
Particle numbers	5
Fittest Bees numbers	5

6. CONCLUSIONS

In this paper, general problems in cooperation in route finding and planning between UAV and ASV are addressed in robotic networks and suggested to be correctly solved. In order to solve this problem, the former cooperation in route finding and planning between UAV and ASV in different complex environments is needed. By came up with a hybrid algorithm, RCGA–APF–CSS, which is a combination of the RCGA, APF, and CSS. According to the simulation results, it was perfect that the proposed hybrid algorithm is more effective than the original algorithms at locating the optimal route of the UAV and ASV within free collision navigation in the environment. The hybrid proposed algorithm in route finding in the UAV reached better results than the RCGA algorithms in terms of route distance 7.22% and iterations 44.4%, and it outperformed the APF algorithm as well, since it improved the route distance and iterations by 10.87% and 33.3%, respectively. Similarly, the hybrid proposed algorithm in route planning in ASV reached enhanced results compared to the RCGA algorithms in distance route 8.06% and iterations 44.4%, and it outdid the APF as well, and then it enhanced the route and iterations by 11.9% and 33.3%, respectively. Moreover, the hybrid proposed algorithm was contrasted with the previous study [24], which used polynomial functions (Polynomial 4th and Polynomial 5th) algorithms applied in a 3D workspace environment, and the proposed algorithm enhanced the route length distance by 27.55% and 51.7%, respectively. Finally, the proposed algorithm was also compared to the ABC-SPPSO [21], which was applied in a 2D workspace environment, which showed improvement in route distance 10.29% and iteration number 9.09%. Upon consideration of the route length of the UAV and ASV compared with the other research, it can be noticed that the proposed hybrid algorithm, the RCGA–APF–CSS algorithm, provided the best combination of shortest route and free-collision navigation within a minimum number of iterations because the proposed algorithm has a great convergence speed, and the algorithm has a trade-off between search and exploitation. In future work, this proposed algorithm method can be used in a swarm of UAVs and ASVs.

REFERENCES

[1] An, X., Wu, C., Lin, Y., Lin, M., Yoshinaga, T., Ji, Y. (2023). Multi-robot systems and cooperative object transport: Communications, platforms, and challenges. IEEE Open Journal of the Computer Society, 4: 23-36. https://doi.org/10.1109/ojcs.2023.3238324

[2] Wu, L.F., Rastgaar, M., Mahmoudian, N. (2024). Heterogeneous multi-robot (UAV-USV-AUV) collaborative exploration with energy replenishment. IFAC-PapersOnLine, 58(20): 159-164. https://doi.org/10.1016/j.ifacol.2024.10.048

[3] Cai, C., Chen, J., Yan, Q., Liu, F. (2022). A multi-robot coverage path planning method for maritime search and rescue using multiple AUVs. Remote Sensing, 15(1): 93. https://doi.org/10.3390/rs15010093

[4] Marques, T., Lima, K., Ribeiro, M., Ferreira, A.S., Sousa, J.B., Mendes, R. (2018). Characterization of highly dynamic coastal environments, employing teams of heterogeneous vehicles: A holistic case study. In 2018 OCEANS-MTS/IEEE Kobe Techno-Oceans (OTO), Kobe, Japan, pp. 1-8. https://doi.org/10.1109/OCEANSKOBE.2018.8559107

[5] Wu, Y., Wang, T., Liu, S. (2024). A review of path planning methods for marine autonomous surface vehicles. Journal of Marine Science and Engineering, 12(5): 833. https://doi.org/10.3390/jmse12050833

[6] Garberoglio, L., Mas, I., Giribet, J.I. (2019). Coordinated ASV-UAV control for marine collision-free navigation. In 2019 XVIII Workshop on Information Processing and Control (RPIC), Salvador, Brazil, pp. 146-151. https://doi.org/10.1109/RPIC.2019.8882141

[7] Woo, J., Lee, J., Kim, N. (2017). Obstacle avoidance and target search of an autonomous surface vehicle for 2016 maritime robotx challenge. In 2017 IEEE Underwater Technology (UT), Busan, Korea (South), pp. 1-5. https://doi.org/10.1109/UT.2017.7890308

[8] D'Amato, E., Nardi, V.A., Notaro, I., Scordamaglia, V. (2021). A visibility graph approach for path planning and real-time collision avoidance on maritime unmanned systems. In 2021 International Workshop on Metrology for the Sea; Learning to Measure Sea Health Parameters (MetroSea), Reggio Calabria, Italy, pp. 400-405. https://doi.org/10.1109/MetroSea52177.2021.9611571

[9] Zhang, H.T., Hu, B.B., Xu, Z., Cai, Z., Liu, B., Wang, X., Geng, T., Zhong, S., Zhao, J. (2021). Visual navigation and landing control of an unmanned aerial vehicle on a moving autonomous surface vehicle via adaptive learning. IEEE Transactions on Neural Networks and Learning Systems, 32(12): 5345-5355.

https://doi.org/10.1109/TNNLS.2021.3080980
[10] Erfianto, B., Adrianne, A., Arif, R.R. (2021). On the experiment of path planning using multi-way points with A* algorithm for autonomous surface vehicle. Kinetik: Game Technology, Information System, Computer Network, Computing, Electronics, and Control, 6(2). https://doi.org/10.22219/kinetik.v6i2.1244
[11] Zhang, J., Wang, Z., Han, G., Qian, Y., Li, Z. (2023). A collaborative path planning method for heterogeneous autonomous marine vehicles. IEEE Internet of Things Journal, 11(1): 1465-1480. https://doi.org/10.1109/JIOT.2023.3289793
[12] Bella, S., Belbachir, A., Belalem, G. (2018). A hybrid architecture for cooperative UAV and USV swarm vehicles. In International Conference on Machine Learning for Networking, pp. 341-363. https://doi.org/10.1007/978-3-030-19945-6_25.
[13] Zhang, H., Zhang, X., Xu, H., Soares, C.G. (2025). Cooperative path following control of USV-UAVs with genetic algorithm extended state observer. Ocean Engineering, 320: 120332. https://doi.org/10.1016/j.oceaneng.2025.120332
[14] Zhu, J., Pan, D. (2024). Improved genetic algorithm for solving robot path planning based on grid maps. Mathematics, 12(24): 4017. https://doi.org/10.3390/math12244017
[15] Li, J., Hu, Y., Yang, S.X. (2025). A novel knowledge-based genetic algorithm for robot path planning in complex environments. IEEE Transactions on Evolutionary Computation, 29(2): 375-389. https://doi.org/10.1109/TEVC.2025.3534026
[16] Iswanto, I., Ma'arif, A., Wahyunggoro, O., Cahyadi, A.I. (2019). Artificial potential field algorithm implementation for quadrotor path planning. International Journal of Advanced Computer Science and Applications, 10(8): 575-585. https://dx.doi.org/10.14569/IJACSA.2019.0100876
[17] Lin, X., Yu, Y.J., Chen, S.Z., Shi, Y.Y. (2023). An improved APF method for complex and dynamic obstacles' avoidance. Unmanned Systems, 11(2): 175-189. https://doi.org/10.1142/S2301385023410054
[18] Lee, H.J., Kim, M.S., Lee, M.C. (2024). Path planning based on artificial potential field with an enhanced virtual hill algorithm. Applied Sciences, 14(18): 8292. https://doi.org/10.3390/app14188292
[19] Peng, B., Zhang, L., Xiong, R. (2024). Smooth path planning with subharmonic artificial potential field. In 2024 International Conference on Advanced Robotics and Mechatronics (ICARM), Tokyo, Japan, pp. 1027-1031. https://doi.org/10.1109/ICARM62033.2024.10715803
[20] Wu, D., Wei, L., Wang, G., Tian, L., Dai, G. (2022). APF-IRRT*: An improved informed rapidly-exploring random trees-star algorithm by introducing artificial potential field method for mobile robot path planning. Applied Sciences, 12(21): 10905. https://doi.org/10.3390/app122110905
[21] Hussein, S.M., Al-Araji, A.S. (2024). Enhancement of a path-finding algorithm for the hovercraft system based on intelligent hybrid stochastic methods. International Journal of Intelligent Engineering & Systems, 17(2): 346-364. https://doi.org/10.22266/ijies2024.0430.29
[22] Yuan, F., Lin, Z., Tian, Z., Chen, B., Zhou, Q., Yuan, C., Huang, Z. (2025). Bio-inspired hybrid path planning for efficient and smooth robotic navigation. International Journal of Intelligent Robotics and Applications, 9: 1934-1964. https://doi.org/10.1007/s41315-025-00479-7
[23] Sang, H., You, Y., Sun, X., Zhou, Y., Liu, F. (2021). The hybrid path planning algorithm based on improved A* and artificial potential field for unmanned surface vehicle formations. Ocean Engineering, 223: 108709. https://doi.org/10.1016/j.oceaneng.2021.108709
[24] Shihab, B.S., Abdullah, H.N., Hassnawi, L.A. (2022). Obstacle avoidance and path planning for UAV using Laguerre polynomial. International Journal of Intelligent Engineering & Systems, 15(6): 657-666. https://doi.org/10.22266/ijies2022.1231.58
[25] Shabalin, D., Stanovov, V. (2025). Neural network-based vehicle control in simulated environments using real-coded genetic algorithms. ITM Web of Conferences, 72: 05008. https://doi.org/10.1051/itmconf/20257205008
[26] Wójcik, K., Ciszkiewicz, A. (2023). Analyzing the performance of real-coded genetic algorithm with control locations for multi-robot path planning. In Polish Conference on Biocybernetics and Biomedical Engineering, pp. 421-430. https://doi.org/10.1007/978-3-031-38430-1_32
[27] Chaoraingern, J., Tipsuwanporn, V., Numsomran, A. (2020). Modified adaptive sliding mode control for trajectory tracking of mini-drone quadcopter unmanned aerial vehicle. International Journal of Intelligent Engineering and Systems, 13(5): 145-158. https://doi.org/10.22266/ijies2020.1031.14
[28] Ghazali, M.H.M., Satar, M.H.A., Rahiman, W. (2024). Unmanned surface vehicles: From a hull design perspective. Ocean Engineering, 312: 118977. https://doi.org/10.1016/j.oceaneng.2024.118977
[29] Kot, R. (2022). Review of collision avoidance and path planning algorithms used in autonomous underwater vehicles. Electronics, 11(15): 2301. https://doi.org/10.3390/electronics11152301
[30] Luis, S.Y., Peralta, F., Córdoba, A.T., del Nozal, Á.R., Marín, S.T., Reina, D.G. (2022). An evolutionary multi-objective path planning of a fleet of ASVs for patrolling water resources. Engineering Applications of Artificial Intelligence, 112: 104852. https://doi.org/10.1016/j.engappai.2022.104852
[31] Kong, F., Wang, Q., Gao, S., Yu, H. (2023). B-APFDQN: A UAV path planning algorithm based on deep Q-network and artificial potential field. IEEE Access, 11: 44051-44064. https://doi.org/10.1109/ACCESS.2023.3273164
[32] Li, W., Tan, M., Wang, L., Wang, Q. (2020). A cubic spline method combing improved particle swarm optimization for robot path planning in dynamic uncertain environment. International Journal of Advanced Robotic Systems, 17(1): 1729881419891661. https://doi.org/10.1177/1729881419891661
[33] Wei, J. (2024). Real-time obstacle avoidance algorithms for unmanned aerial and ground vehicles. Master's thesis, University of New South Wales (Australia). https://doi.org/10.26190/unsworks/30514
[34] Sadat, N., Dai, R. (2025). A survey of quality-of-service and quality-of-experience provisioning in information-centric networks. Network, 5(2): 10. https://doi.org/10.3390/network5020010
[35] Lu, Y., Zhang, S., Liu, C., Zhang, R., Ai, B., Niyato, D., Ni, W., Wang, X., Jamalipour, A. (2025). Agentic graph

neural networks for wireless communications and networking towards edge general intelligence: A survey. arXiv preprint arXiv:2508.08620. https://doi.org/10.48550/arXiv.2508.08620